Modification of SO_4^{2-}–ZrO_2 and Pt/SO_4^{2-}–ZrO_2 properties during *n*-hexane isomerization

S.R. Vaudagna, R.A. Comelli and N.S. Fígoli

Instituto de Investigaciones en Catálisis y Petroquímica – INCAPE (FIQ-UNL, CONICET), Santiago del Estero 2654, 3000 Santa Fe, Argentina
E-mail: nfigoli@fiqus,unl.edu.ar

Received 17 April 1997; accepted 12 July 1997

The modification of the textural properties and crystalline structure of SO_4^{2-}–ZrO_2 and Pt/SO_4^{2-}–ZrO_2 during *n*-hexane reaction at 473 K and 6 kg cm^{-2} has been studied in the presence of either hydrogen or nitrogen. Sulfur content before and after reaction and the amount of coke at the end of the reaction were measured. The coke deposited on the catalysts blocks the pores of small size and decreases the surface area of the used catalysts. After regeneration, surface area is not completely restored. The loss of sulfur during reaction, probably associated to the reaction medium, also produces a decrease in surface area by the collapse of the smallest pores which generates larger ones. The transformation of tetragonal to monoclinic crystalline structure of zirconia begins to occur when sulfur content drops below a critical value.

Keywords: sulfated zirconia, platinum sulfated zirconia, textural properties, crystalline structure, *n*-hexane isomerization

1. Introduction

Sulfate-promoted zirconia is a well known alkane isomerization catalyst. Most of the studies related to this catalyst have been carried out taking the isomerization of *n*-butane and *n*-pentane as test reactions [1–4]. The addition of a metal improves catalyst stability and also modifies catalyst selectivity; different catalytic behaviors have been found when the reaction is performed in the presence of hydrogen [5–7].

It is well known that zirconium hydroxide sulfation produces important modifications in the surface area and crystalline structure of zirconia. Sulfated zirconia has a larger surface area than pure zirconia when both materials have been calcined at high temperatures [2,8–10], because sulfation partly preserves the high surface area of zirconium hydroxide and also retards the transition from an amorphous material to a crystalline one [8,11,12].

The effect of different preparation parameters such as zirconium precursor and reaction media [12,13], pH [14], precipitation and sulfating agents [8,15], sulfur concentration and calcination temperature [15,16] on the textural properties and crystalline structure of sulfated zirconia, have been widely studied. Although sulfated zirconia deactivation has been reported [17–19], there are no references regarding the modifications of either textural properties or crystalline structure during reaction. The objective of this paper is to study the modifications of the textural properties and crystalline structure of SO_4^{2-}–ZrO_2 (SZ) and Pt/SO_4^{2-}–ZrO_2 (PtSZ) during the *n*-hexane reaction carried out in the presence of either hydrogen or nitrogen.

2. Experimental

2.1. Catalyst preparation

$Zr(OH)_4$ was prepared from an aqueous solution containing 11% zirconium oxychloride octahydrate (Strem Chemicals, 99.9%) by dropwise addition of an ammonium hydroxide solution (Merck, 25% ammonia) up to pH 10. More details about the preparation technique were previously reported [20]. $Zr(OH)_4$ has a BET specific surface area of 328 $m^2\ g^{-1}$ and a pore volume of 0.22 $cm^3\ g^{-1}$. The platinum was added impregnating the $Zr(OH)_4$ by the incipient wetness technique using a $H_2PtCl_6 \cdot 6H_2O$ solution with the adequate concentration to obtain 0.5% platinum on the solid. This material was dried at 383 K for 12 h. Sulfate was added by dipping the dried $Zr(OH)_4$, with or without platinum, in a 0.5 M sulfuric acid solution for 1 h without stirring and with 2.2 $cm^3\ g^{-1}$ acid solution/solid ratio. These sulfated samples were filtered and dried at 383 K for 12 h.

2.2. Catalyst characterization

Platinum concentration was measured by inductively coupled plasma atomic emission spectrometry (ICP-AES) using a Perkin-Elmer ICP/5500 plasma spectrometer and sulfur by combustion in a LECO CS-244 analyzer. Acidity was measured by ammonia temperature-programmed desorption, as previously described [20]. The used catalysts were regenerated at 500°C for 3 h before the TPD experiment.

The catalyst texture was measured using a Micromeritics Accusorb 2100 equipment; samples were

previously degassed in vacuum at 383 K for 2 h. From the nitrogen adsorption isothermal data, the BET specific surface area (S_g), cumulative pore volume (V_g), Wheeler mean pore diameter (D_w) and pore diameter distribution, were calculated. Crystalline structure was analyzed by X-ray diffraction with a Shimadzu XD-D1 equipment using Cu Kα radiation, /2/2/0.6 windows and a scan of 0.125° min^{-1}. Measurements were made in the 26°–33° 2θ range where the most important peaks corresponding to tetragonal and monoclinic crystalline structure of zirconia appear. Peaks deconvolution was made using the option "profile fitting" of the DP-D1 system software.

Catalytic activity and selectivity for the *n*-hexane isomerization reaction were measured in a flow fixed-bed tubular reactor. The stainless-steel reactor had 18 mm internal diameter and 1 g of catalyst sieved to 35–80 mesh was charged for the test. Catalysts were calcined 3 h at 873 K in an air stream and cooled overnight to room temperature in a nitrogen flow. The reaction was performed by feeding *n*-hexane (Merck p.a.) during 9 or 360 min at 473 K, 6 kg cm^{-2}, 4 h^{-1} weight hourly space velocity, and hydrogen/*n*-hexane or nitrogen/*n*-hexane molar ratio of 6. Mass transfer limitations were absent under the experimental conditions used. Special attention was given to the first minutes on stream, collecting product samples in a 16-port multiloop sampling valve. *n*-hexane and reaction products were analyzed by on-line gas chromatography using a 100 m long, 1/16 in. o.d. column packed with squalene, operated isothermally at 308 K. Carbon content was measured by combustion in a specially designed equipment in order to improve both sensitivity and resolution [21].

3. Results

Catalytic activity and selectivity of SZ run with nitrogen (SZN_2) or hydrogen (SZH_2) and of PtSZ run with nitrogen ($PtSZN_2$) or hydrogen ($PtSZH_2$) are shown in table 1. The last catalyst shows a good activity and stability with a high selectivity to C_6 products, mainly C_6 isomers; the other three samples show, at 3 min-on-stream, both high activity and selectivity to cracking products but they are almost completely deactivated after 9 min-on-stream. Details about the reaction mechanism (which is different for $PtSZH_2$ than for the other catalysts) have been published [19,22]. The distribution of the C_6 isomerization products is presented in table 2. The differences in selectivity for $PtSZH_2$ and the other catalysts are due to differences in the reaction mechanism [19,22]. For $PtSZH_2$, the high isomerization selectivity can be explained considering that platinum heterolytically dissociates hydrogen, generating hydrides, as proposed by Iglesia et al. [6]. The hydride interacts with intermediate carbenium ions, giving the isomeric hexanes. When hydrides are not preset ($PtSZN_2$, SZH_2 and SZN_2), the carbenium ions remain long time at the surface, they are either oligomerized and then cracked or polymerized into coke. In the C_6 fraction, methylpentanes are the main reaction products and dimethylbutanes are produced in lower amounts. Methylcyclopentane and cyclohexane are practically only produced over SZN_2, SZH_2 and $PtSZN_2$, being more noticeable for $PtSZN_2$. Cracking products distribution is similar for all samples and times-on-stream: only C_3–C_5 are produced, isobutene being the main one.

The textural properties and sulfur content of only calcined catalysts and after being run in the *n*-hexane reaction under nitrogen or hydrogen atmospheres for either 9 or 360 min, and the carbon content of the used catalysts, are presented in table 3. An important decrease of S_g with time is observed for SZN_2 and SZH_2, without important modifications of V_g, except for SZN_2 run during 360 min. Although both samples showed similar S_g at 9 min, the decrease is higher for SZN_2 run for 360 min. PtSZ, run either with nitrogen or hydrogen, shows a similar behavior. Comparing SZ and PtSZ, it can be seen that SZN_2 used for 360 min has a lower S_g than $PtSZN_2$ used during the same time. The decrease in S_g with time for SZH_2 and $PtSZH_2$ is the same. The regeneration with air at 773 K for 180 min of $PtSZN_2$ used for 360 min and $PtSZH_2$ used for 9 min produces the recovery of an important fraction of the S_g of the only calcined sample, while SZN_2 used during 360 min, after regeneration shows only a small recovery of S_g.

Regarding coke deposition on SZ, it can be seen that

Table 1
Activity (moles of *n*-hexane converted (moles of sulfur)$^{-1}$ h^{-1}) and selectivity to C_6 products (S_{C_6}) and to cracking products (S_{cr}) at two times-on-stream for different samples

Sample	Activity		S_{C_6} (%)		S_{cr} (%)	
	3 min	300 min	3 min	300 min	3 min	300 min
SZN_2	46.1	0.4	31	100	69	0
SZH_2	47.2	0.7	33	100	67	0
$PtSZN_2$	51.9	0.5	32	100	68	0
$PtSZH_2$	66.1	56.0	96	97	4	3

Table 2
Product distribution in the C_6 fraction for SZ and PtSZ run with N_2 or H_2 for two times-on-stream

Catalyst	Time (min)	2MP (%)	3MP (%)	2,3DMB (%)	2,2DMB (%)	MCP (%)	CH (%)
SZN_2	6	51.8	29.9	14.8	3.5	0	0
	300	44.8	30.1	10.8	0	11.2	3.1
SZH_2	6	51.8	29.3	14.2	3.4	0.4	0.9
	300	45.6	30.0	10.0	0.9	10.5	3.0
$PtSZN_2$	6	53.8	29.1	12.6	2.6	0.5	1.4
	300	10.1	40.1	0	0	49.8	0
$PtSZH_2$	6	46.7	27.9	12.2	13.1	0.1	0
	300	47.0	29.0	12.0	12.0	0	0

Table 3
Textural properties and sulfur content of only calcined and used catalysts and carbon content of used catalysts run during 9 or 360 min

Catalyst	Time (min)	S_g ($m^2\ g^{-1}$)	V_g ($cm^3\ g^{-1}$)	D_w (nm)	C (wt%)	S (wt%)
SZ [a]	0	122	0.100	3.2	0	2.2
SZN_2	9	97	0.100	3.9	0.17	1.4
SZN_2	360	65	0.086	5.3	0.25	1.0
SZH_2	9	100	0.095	3.8	0.19	1.4
SZH_2	360	92	0.095	4.3	0.27	1.3
PtSZ [a]	0	122	0.103	3.4	0	1.8
$PtSZN_2$	9	94	0.101	4.3	0.14	1.6
$PtSZN_2$	360	78	0.082	4.2	1.23	1.5
$PtSZH_2$	9	100	0.102	4.0	0.04	1.6
$PtSZH_2$	360	92	0.101	4.4	0.92	1.3
$PtSZN_2$ [b]	–	113	0.104	3.7	0	n.a. [d]
$PtSZH_2$ [c]	–	111	0.110	4.2	0	n.a.
SZN_2 [b]	–	74	0.100	5.4	0	n.a.

[a] Only calcined.
[b] Sample used during 360 min and then regenerated at 773 K for 180 min.
[c] Sample used during 9 min and then regenerated at 773 K for 180 min.
[d] Not available.

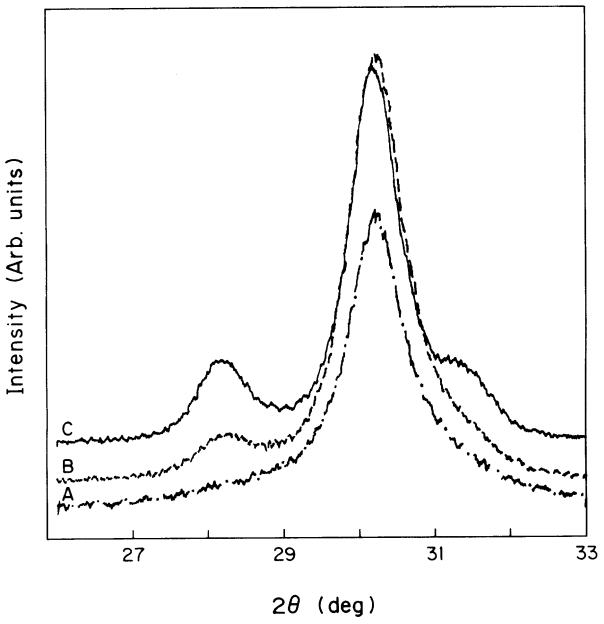

Figure 1. X-ray diffraction spectra of different samples: (A) (– · –) SZ (only calcined); (B) (– – –) SZN_2 run for 9 min; (C) (———) SZN_2 run for 360 min.

there are no important differences between the samples used in nitrogen or hydrogen during 9 or 360 min. For $PtSZN_2$ and $PtSZH_2$, a larger amount of coke is observed after 360 min. When both platinum and hydrogen are present, the amount of coke is smaller at short times-on-stream, but is larger at longer times, when compared with SZH_2 or SZN_2.

Table 3 also shows the sulfur content of only calcined and used catalysts. There exists a more important loss of sulfur during the first minutes of the run, the decrease being higher for the SZ samples than for the PtSZ ones. Figure 1 shows the 26°–33° 2θ range XRD pattern for different samples, in order to analyze the crystalline structure of zirconia. SZ (only calcined) presents only one peak centered at $2\theta = 30.2°$ corresponding to the tetragonal phase [23]. SZN_2, used for 9 min in the *n*-hexane reaction, shows a peak at $2\theta = 28.2°$, attributed to the monoclinic phase of zirconia, in addition to the peak characteristic of tetragonal zirconia. The peak corresponding to monoclinic zirconia increases with time-on-stream and another peak at 31.5°, also corresponding to the monoclinic phase, appears in SZN_2 run for 360 min. A similar qualitative behavior was observed for the other samples. The volume fraction (V_m) of the monoclinic phase of zirconia calculated using the nonlinear relationship reported by Mercera et al. [24] is presented in table 4; it was determined from the intensity of the peaks at $2\theta = 28.2°$, 31.5° and 30.2°. The volume fraction of the monoclinic phase increases with time-on-stream for SZN_2; a similar behavior is presented by the other samples. Samples with almost the same sulfur content (SZN_2 run for 9 min, SZH_2 and $PtSZH_2$ run for 360 min) present a similar volume fraction of the monoclinic phase.

Figure 2 presents the pore size distribution for SZ (only calcined), SZN_2 run for 9 and 360 min, and the last sample after regeneration in air at 773 K for 180 min. After 9 min, the disappearance of a fraction of small pores has occurred; the maximum of the dV/dD function has been shifted towards larger pores. A more noticeable effect is observed after 360 min-on-stream; the area under the curve is smaller, thereby indicating a smaller pore volume. Only a small recovery of the small pores and a broader profile is observed after regeneration.

Figure 3 shows the pore size distribution of PtSZ (only calcined), $PtSZN_2$ used for 360 min and after its regeneration in air at 773 K for 180 min; it is noticeable that after regeneration, only a fraction of the small pores is recovered. The pore size distributions corresponding to SZH_2 and $PtSZH_2$ run during 9 and 360 min show a similar behavior.

Ammonia temperature-programmed desorption patterns of fresh SZ and PtSZ, as well of the last one after being used in the *n*-hexane reaction in the presence of nitrogen or hydrogen and regenerated are presented in figure 4. Fresh SZ presents only one desorption peak,

Table 4
Volume fraction of the monoclinic phase of zirconia (V_m) for different catalysts

	Catalyst					
	SZ [a]	SZN_2 [b]	SZN_2 [c]	SZH_2 [c]	PtSZ [a]	$PtSZH_2$ [c]
V_m	0	0.20	0.65	0.26	0	0.25

[a] Only calcined.
[b] Sample used during 9 min.
[c] Sample used during 360 min.

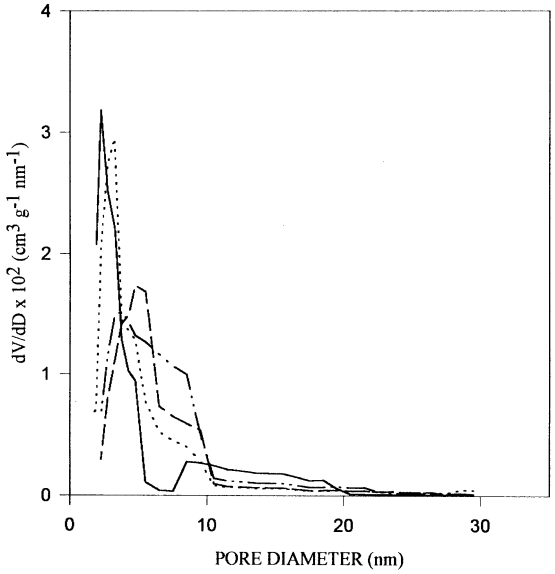

Figure 2. Pore size distribution of several SZ samples: (———) only calcined SZ; (· · ·) SZN_2 run during 9 min; (– – –) SZN_2 run during 360 min; (–·–·–) SZN_2 run during 360 min and then regenerated in air at 773 K.

while PtSZ presents two desorption peaks in the profile. PtSZ used with hydrogen or nitrogen and regenerated shows practically the same profile as the only calcined sample.

4. Discussion

The lower surface area after reaction may indicate that the blockage of a fraction of pores has occurred due to coke accumulation. Nevertheless, we have not found

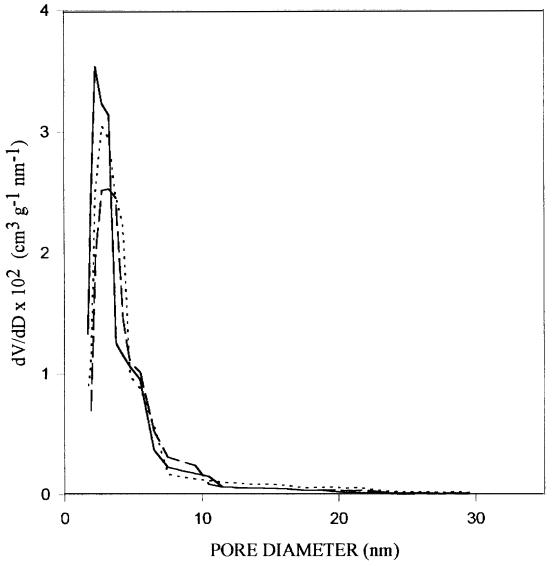

Figure 3. Pore size distribution of PtSZ samples: (———) PtSZ only calcined; (– – –) $PtSZN_2$ run during 360 min; (· · ·) $PtSZN_2$ run during 360 min and then regenerated in air at 773 K.

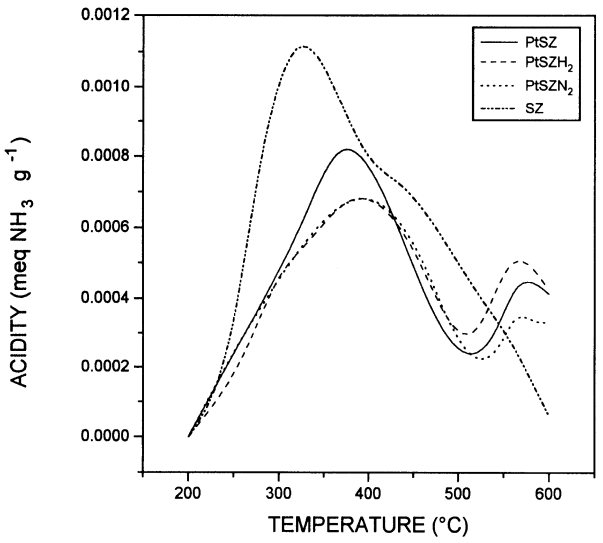

Figure 4. Ammonia temperature-programmed desorption profiles of several samples.

a direct relationship between the amount of coke and the decrease in surface area. SZN_2 has lower S_g and similar carbon content than SZH_2, both run during 360 min. Comparing SZH_2 and $PtSZH_2$ run for 360 min, it can be seen that they have the same S_g (92 m^2 g^{-1}) but different carbon content (0.27 and 0.92%, respectively). The coke deposition, after 360 min-on-stream is higher for the platinum containing samples, which can be explained by considering the dehydrogenating capacity of platinum, as it has also been found comparing Al_2O_3 and Pt/Al_2O_3 [25]. We have previously considered a different reaction path for SZN_2, SZH_2 and $PtSZN_2$ than for $PtSZH_2$, showing that coke with a different degree of condensation is produced according to these paths [19].

The pore size distribution of $PtSZN_2$ run during 360 min changes after regeneration (figure 3); the difference of the dV/dD function in the region of the smallest pores (which are those that contribute more to S_g) indicates that coke deposition produces the blockage of those pores. The regeneration of $PtSZN_2$ and $PtSZH_2$ used during 360 and 9 min, respectively, in spite of the total coke elimination, do not have a complete S_g recovery. Then, another phenomenon occurs at the same time. Considering the pore size distribution of the SZN_2 samples shown in figure 2, it can be observed that, after reaction, the maximum of the dV/dD function is shifted to larger pores. SZ has 2.2% sulfur content while SZN_2 after being run with nitrogen for 9 or 360 min has 1.4% and 1.0%, respectively. We can consider that, as a consequence of the sulfur loss (nearly 50%) during the reaction, there occurs a collapse of a fraction of the smallest pores, resulting in the formation of larger ones, with the corresponding decrease in surface area and pore volume. The shift to larger pores for $PtSZN_2$ is less noticeable because the loss of sulfur was lower than for SZN_2. It has been reported [8–10,15] that sulfur partly preserves the

smallest pores and surface area of $Zr(OH)_4$ after calcination at high temperatures. Chen et al. [16] reported results of specific surface area of SZ as a function of percentage of sulfur for samples calcined at 773 or 873 K; they observed an important increase of the surface area (about 100%) for sulfur concentrations between 0 and 2%. It is within this range of sulfur concentrations that our samples have lost between 17 and 50% sulfur. Then, we can assume that the decrease in surface area during reaction is due to the blockage of small pores by coke and to their collapse due to the loss of sulfur.

The preservation of the surface area and the stabilization of the tetragonal phase are related phenomena [24]. Two interpretations have been proposed for SZ. Srinivasan et al. [11] considered that oxygen from the gas phase is adsorbed on surface sites of zirconia, favoring the transformation from the tetragonal to the monoclinic phase; the presence of sulfate allows to keep these sites, inhibiting the transformation in the presence of oxygen. Norman et al. [9] considered that the stabilization of the surface area and of the tetragonal structure is due to the higher thermal stability of the sulfate bridges than of the hydroxyl bridges and to the increase of the Zr–Zr distance produce by sulfate, in addition to the prevention of diffusive processes due to the largest rigidity induced by the sulfate bridges over the structure of zirconia. The sulfur content (related to the sulfation technique and the calcination temperature used) has strong incidence over the crystalline phase obtained after calcination. PtSZ and SZ, with 1.8 and 2.2% sulfur, respectively, show only tetragonal phase after calcination at 873 K (table 3) while samples without Pt, sulfated using another method and with about 1% sulfur, present both tetragonal and monoclinic phases after calcining at 873 K [12]. Chen et al. [16] reported that SZ, having 1.8% sulfur after calcination at 773 K, presents only the tetragonal crystalline phase of zirconia, whereas the same sample shows both tetragonal and monoclinic phases when the sulfur content decreases to 1.2% by calcination at 873 K. Yamaguchi et al. [8] observed the monoclinic phase of zirconia on SZ from 1073 K while sulfur decreases from 923 K. We have observed a loss of sulfur during reaction for all samples. Sulfur is present mainly as S^{6+} species on SZ and PtSZ surfaces [20,26] and the reduction of these species in the presence of hydrogen and/or platinum is not expected at our reaction temperature, 473 K [26,27]; then, the sulfur loss might be related to the reaction media, as proposed by Ng and Horvát [17]. These results allow us to consider that the loss of sulfur below a critical value induces the transformation of the tetragonal to the monoclinic crystalline phase of zirconia. Although the loss of sulfur, the modifications in the textural properties and the appearance of the monoclinic phase of zirconia are qualitatively the same for the two catalysts either in the presence of hydrogen or nitrogen, the acidity as measured by ammonia thermal-programmed desorption, does not change significantly after the catalysts have been used and regenerated. This is an indication that the presence of hydrides in the reaction media, as happens in the case of $PtSZH_2$, is the reason of the preservation of the activity.

5. Conclusions

Coke deposited during the *n*-hexane reaction decreases the surface area of SZ and PtSZ by blockage of the small-diameter pores. Regeneration, in spite of the total coke elimination, does not produce a complete surface area recovery. The sulfur loss during the reaction also contributes to the decrease in surface area, generating larger pores by the collapse of the smallest ones. A transition from the tetragonal to the monoclinic crystalline phase of zirconia occurs during reaction at 473 K when the sulfur content drops below a critical value.

Acknowledgement

This study was carried out within a JICA-CENACA project. The financial assistance of CAI+D (UNL) is acknowledged.

References

[1] M. Hino and K. Arata, J. Chem. Soc. Chem. Commun. (1980) 851.
[2] K. Arata, Adv. Catal. 37 (1990) 165.
[3] B.H. Davis, R.A. Keogh and R. Srinivasan, Catal. Today 20 (1994) 219.
[4] X. Song and A. Sayari, Catal. Rev. Sci. Eng. 38 (1996) 329.
[5] K. Ebitani, J. Konishi and H. Hattori, J. Catal. 130 (1991) 257.
[6] E. Iglesia, S.L. Soled and G.M. Kramer, J. Catal. 144 (1993) 238.
[7] F. Garin, D. Andriamasinoro, A. Abdulsamad and J. Sommer, J. Catal. 131 (1991) 199.
[8] T. Yamaguchi, K. Tanabe and Y.C. Kung, Mater. Chem. Phys. 16 (1986) 67.
[9] C.J. Norman, P.A. Goulding and I. McAlpine, Catal. Today 20 (1994) 313.
[10] S.R. Vaudagna, R.A. Comelli and N.S. Fígoli, React. Kinet. Catal. Lett. 58 (1996) 111.
[11] R. Srinivasan, T.R. Watkins, C.R. Hubbard and B.H. Davis, Chem. Mater. 7 (1995) 725.
[12] R.A. Comelli, C.R. Vera and J.M. Parera, J. Catal. 151 (1995) 96.
[13] R. Srinivasan and B.H. Davis, Catal. Lett. 14 (1992) 165.
[14] A. Corma, V. Fornés, M.I. Juan-Rajadell and J.M. Nieto, Appl. Catal. A 116 (1994) 151.
[15] J.M. Parera, Catal. Today. 15 (1992) 481.
[16] F.R. Chen, G. Coudurier, J.F. Joly and J.C. Vedrine, J. Catal. 143 (1993) 616.
[17] F.T.T. Ng and N. Horvát, Appl. Catal. A 123 (1995) L197.
[18] D. Spielbauer, G.A.H. Mekhemer, E. Bosch and H. Knözinger, Catal. Lett. 36 (1996) 59.
[19] S.R. Vaudagna, R.A. Comelli, S.A. Canavese and N.S. Fígoli, J. Catal., in press.

[20] R.A. Comelli, S.A. Canavese, S.R. Vaudagna and N.S. Fígoli, Appl. Catal. A 135 (1996) 287.
[21] S.C. Fung and C.A. Querini, J. Catal. 138 (1992) 240.
[22] R.A. Comelli, Z.R. Finelli, S.R. Vaudagna and N.S. Fígoli, Catal. Lett. 45 (1997) 227.
[23] *Selected Powder Diffraction Data for Metals and Alloys*. Data Book, 1st Ed., Vol. II, cards No. 13-307 and No. 24–1164, Joint Committee on Powder Diffraction Standards (JCPDS), Swarthmore, USA.
[24] P.D.L. Mercera, J.G. Van Ommen, E.B.M. Doesburg, A.J. Burggraaf and J.R.H. Ross, Appl. Catal. 57 (1990) 127.
[25] J.M. Parera, N.S. Fígoli, G.E. Costa and M.R. Sad, React. Kinet. Catal. Lett. 22 (1983) 231.
[26] K. Ebitani, H. Konno, T. Tanaka and H. Hattori, J. Catal. 135 (1992) 60.
[27] T. Hosoi, T. Shimidzu, S. Itoh, S. Baba and H. Takahoka, in: *Symp. on Preparation and Characterization of Catalysts*, ACS Petroleum Chemistry Division, Vol. 33 (1988) 562.